Supporting Information

Unraveling the Solvent Induced Welding of Silver Nanowires for High Performance Flexible Transparent Electrodes

Kui Zhang,[†] *Jia Li,*[†] *Yunsheng Fang,*[†] *Beibei Luo, Yanli Zhang, Yanqiu Li, Jun Zhou, and Bin Hu**

Wuhan National Laboratory for Optoelectronics and School of Optical and Electronic Information, Huazhong University of Science and Technology, Wuhan 430074, China

[†]These authors contributed equally to the work.

* Correspondence author: bin.hu@hust.edu.cn

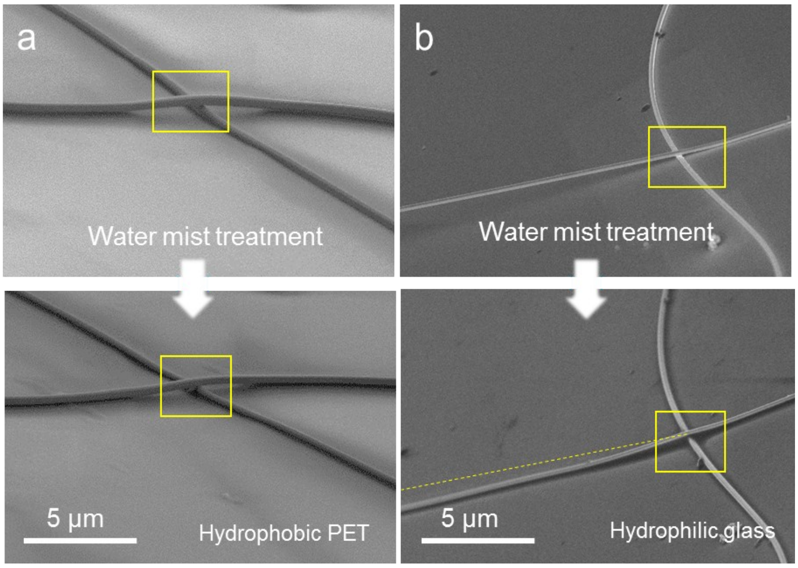

Figure S1. Lower magnification SEM images of AgNWs wire-wire junctions before and after water-mist treatment on (a) glass and (b) PET substrates. Yellow squares show the magnified areas in Figure 1c, 1d, yellow dash line marks the original position of the cocked AgNW before water-mist treatment.

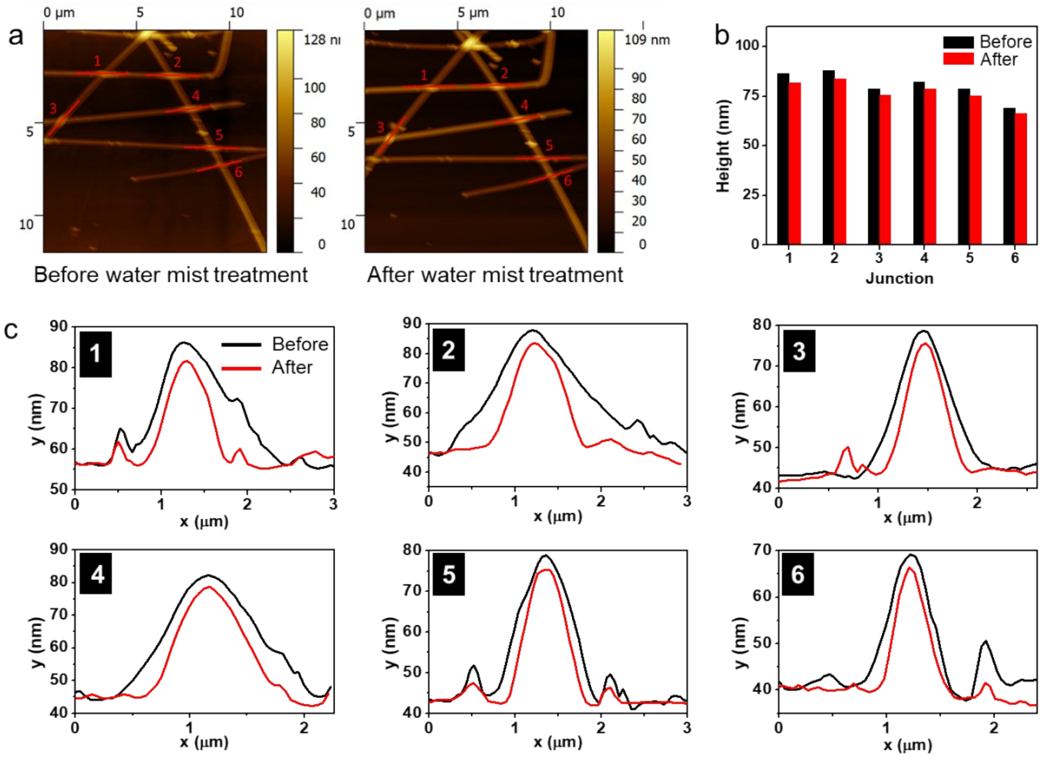

Figure S2. Changes in height and width of AgNWs junctions before and after water-mist treatment on glass substrate. (a) AFM images before and after water-mist treatment. (b) Changes in height of AgNWs junctions shown in (a). (c) The detailed change in height and width of the six AgNWs junctions marked in (a) with red lines.

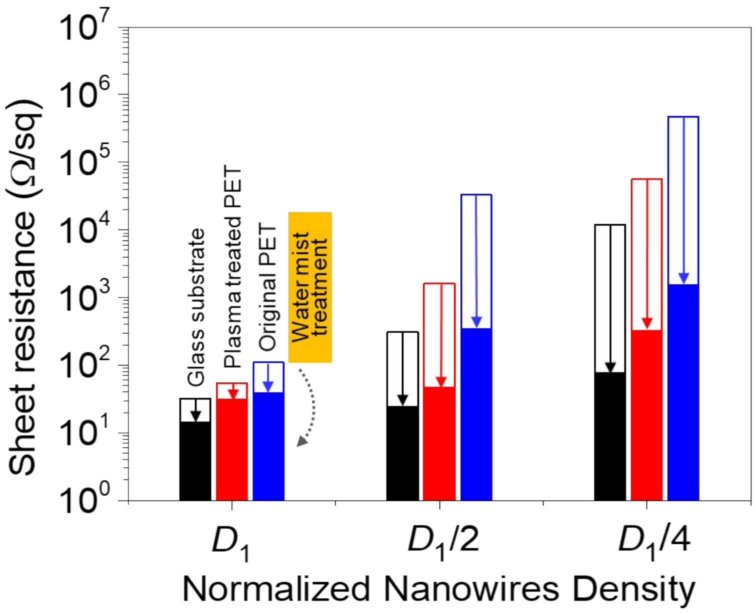

Figure S3. Effect of water-mist treated ultrathin AgNWs TEs on different substrates. Changes of R_s before (blank) and after (solid) water-mist treatment of AgNWs TEs on different substrates (glass: black, plasma-treated PET: red, and PET without treatment: blue), three different concentration inks were used to control the initial AgNWs density (D_1 = 0.08 mg/cm^2).

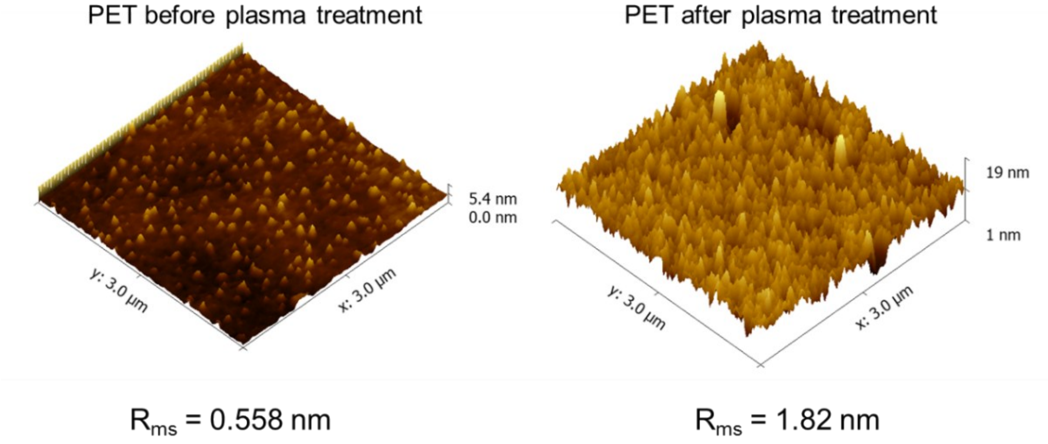

Figure S4. AFM scanning image of PET substrate surfaces before (a) and after (b) air plasma treatment. The average roughness (R_{ms}) was measured to be 0.558 nm in original PET, and increased to 1.82nm after treatment.

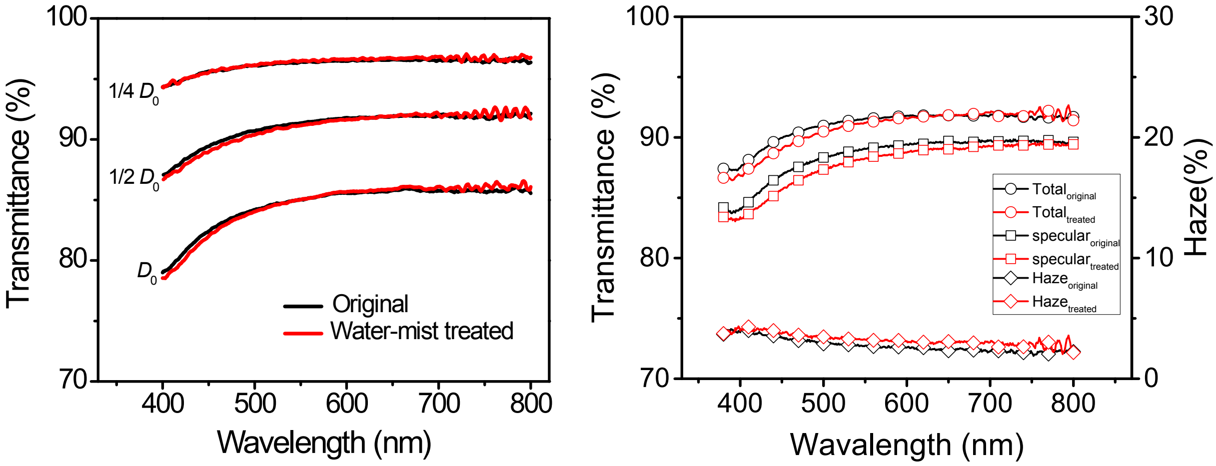

Figure S5. (a) The total optical transmittance spectra of the as-prepared (black curves) and water-mist treated (red curves) AgNWs TE on glass substrate, respectively, which show a negligible change in transmission. The same samples were used in Figure 3a. ($D_0 = 0.12$ mg/cm^2) (b) The total (circle), specular (square) transmittance spectra and haze (diamond) of the as-prepared (black curves) and water-mist treated (red curves) AgNWs TE on glass substrate.

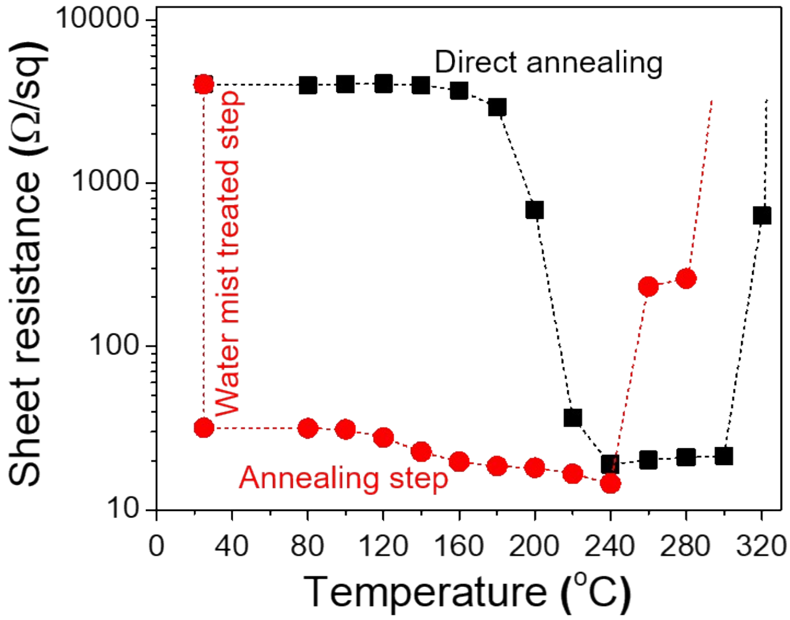

Figure S6. The comparison of welding effect between thermal annealing and water-mist treatment. Two AgNWs TEs on glass substrates with the same size of 2.5 cm × 2.5 cm and similar initial R_s of 4027 Ω (first black dot) and 4015 Ω (first red dot), respectively, the latter was treated with water-mist at room temperature and the R_s immediately dropped to 31.6 Ω which was similar to the thermal-treated sample at 220 °C (36.7 Ω). Heating condition: the hot plate was set to hold at different temperature of 80, 100, 120, 140, 160, 180, 200, 220, 240, 260, 280, 300 and 320 °C, respectively, and each stage for 10 min. At every temperature stage, R_s was measured after the samples cooling to room temperature.

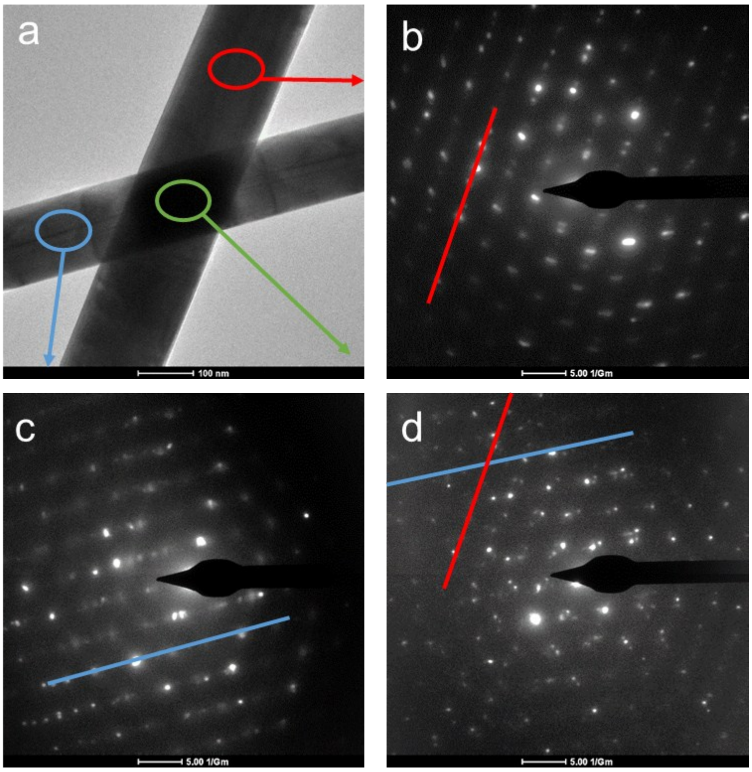

Figure S7. HRTEM analysis of water-mist treated AgNWs junction (a) HRTEM image of the AgNWs junction. (b~d) selected area electron diffraction (SAED) patterns from various locations that are labeled in (a). The SAED pattern on the junction (d) is quite similar to the simple overlap of the patterns from each individual AgNW (b and c). The AgNWs maintain their own crystalline directions after the water-mist treatment, which indicate that the cold-welding phenomenon is a very localized and superficial process, without involving any change in the bulk of AgNW.

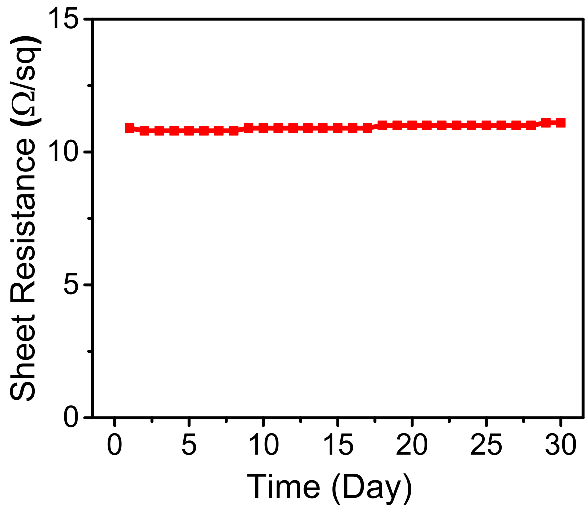

Figure S8. The stability of AgNWs TE after water-mist treatment.

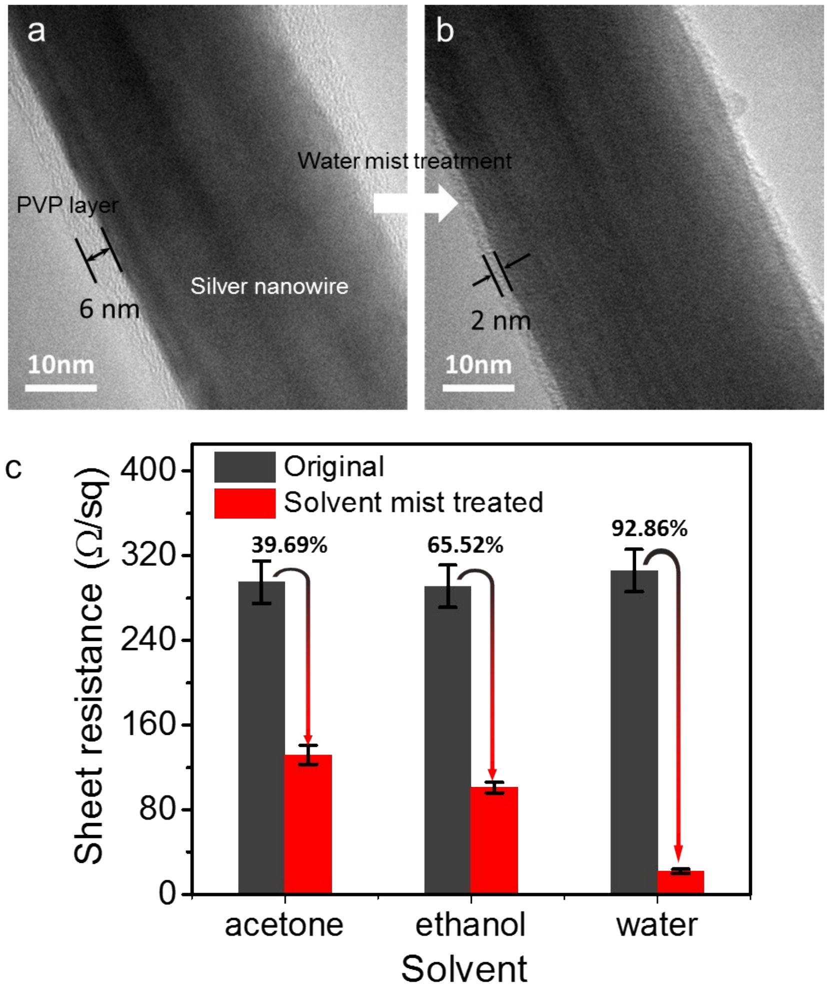

Figure S9. Effect of solvents on the R_s of the ultrathin AgNWs electrodes. TEM images of the PVP layer on the AgNWs before (a) and after (b) water-mist treatment. (c) Relative changes in R_s (R_0 - R/R_0 × 100%) of the AgNW TEs on glass substrate with different solvent-mist treatments. (The length and diameter of the ultrathin AgNW were ~50μm and ~35nm, respectively.)

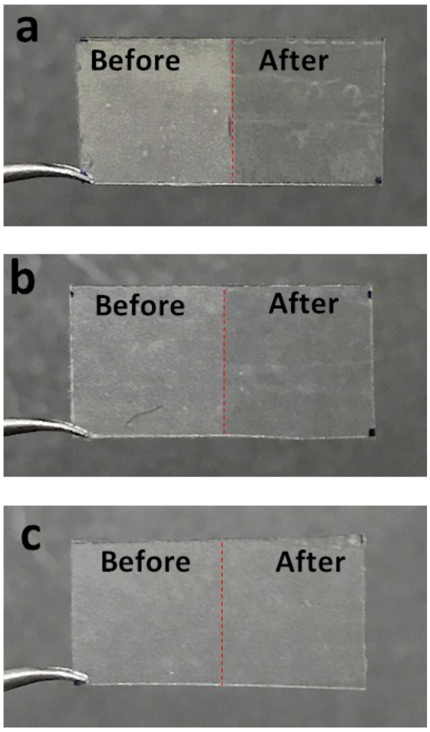

Figure S10. Photographs of three types of AgNWs TEs on PET substrates using tape test (a) original PET substrate without any treatment, (b) original PET substrate with water-mist treatment and (c) plasma-treated PET substrate with water-mist treatment. The red dash lines show the tape-peeling boundaries.

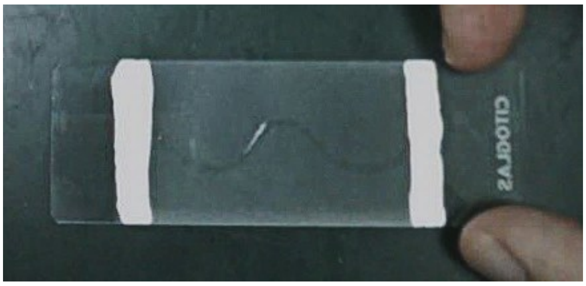

Figure S11. Photograph of the AgNWs TE after water-mist patterning but before the complete evaporation of water path.

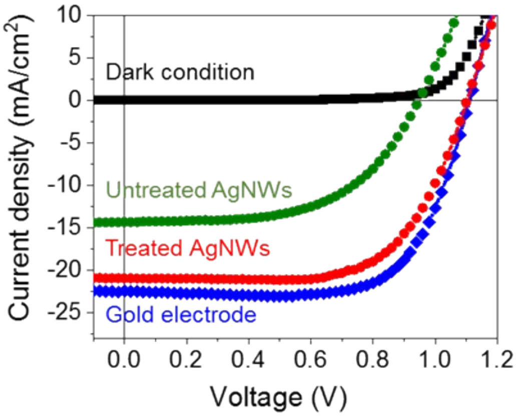

Figure S12. Performance of perovskite solar cell with untreated AgNWs/ PDMS transparent electrode, water-mist treated AgNWs/PDMS transparent electrode and reference gold electrode.

The water mist treated AgNW TE can be as the top electrode of the perovskite solar cell, structure of the solar cell was FTO/TiO_2/perovskite/2,2′,7,7′ tetrakis (*N*,*N*di*p*methoxyphenylamine) 9,9′-spirobifluorene(Spiro OMeTAD)/poly (3,4 ethylene dioxythiophene) :polystyrenesulfonate) (PEDOT:PSS)/ AgNWs (or gold electrodes). The current density-voltage (*J-V*) curves of the solar cell with the welding AgNW TE, when illuminated from bottom side (FTO side), the short-circuit current density (J_{sc}), open-circuit voltage (V_{oc}), and fill factor (FF) were 20.68 mA cm^{-2}, 1.10V, and 0.674, respectively.

Table S1. Summarized the TEs performance by utilizing different cold-welding methods

Methods	Transmission(T) (%)	Sheet resistance(Rs) (Ω sq−1)	References
High static pressure	80~87	11~15	[1]
Supersonic spraying	80~90	3~10	[2]
Electrical annealing	86.70	19.7	[3]
Plasmonic welding	95	580	[4]
Electron beam irradiated	88.80	48	[5]
Chemical welding	95	-	[6]
This work	80~95	5~34	

Table S2. Surface tension and PVP solubility of different solvent

Solvent	Surface Tension (mN/m)	PVP Solubility
Water (25 ^{o}C)	71.99	Soluble
Ethanol (25 ^{o}C)	21.8	Soluble
Acetone (25 ^{o}C)	24.0	Insoluble

Table S3. Performance of perovskite solar cell with AgNWs TEs and reference opaque gold-electrode solar cell with the same structure.

Electrodes	V_{OC} [V]	J_{sc} [mA•cm^{-2}]	*FF* [%]	*PCE* [%]
Untreated AgNWs	0.95	14.3	57.1	7.7
Treated AgNWs	1.10	20.68	67.4	15.3
Opaque gold	1.11	22.42	71.9	17.9

References

[1] T. C. Hauger, S. I. Al-Rafia, J. M. Buriak, *ACS Appl. Mater. Interfaces* **2013**, *5*, 12663-12671.

[2] J.-G. Lee, D.-Y. Kim, J.-H. Lee, S. Sinha-Ray, A. L. Yarin, M. T. Swihart, D. Kim, S. S. Yoon, *Adv. Funct. Mater.* **2017**, 27.1

[3] T.-B. Song, Y. Chen, C.-H. Chung, Y. Yang, B. Bob, H.-S. Duan, G. Li, K.-N. Tu, Y. Huang, Y. Yang, *ACS Nano* **2014**, 8, 2804-2811.

[4] E. C. Garnett, W. Cai, J. J. Cha, F. Mahmood, S. T. Connor, M. Greyson Christoforo, Y. Cui, M. D. McGehee, M. L. Brongersma, *Nat. Mater.* **2012**, *11*, 241-249.

[5] C. H. Hong, S. K. Oh, T. K. Kim, Y. J. Cha, J. S. Kwak, J. H. Shin, B. K. Ju, W. S. Cheong, *Sci. Rep.* **2015**, 5, 17716.

[6] S. S. Yoon, D. Y. Khang, *Nano Lett.* **2016**, *16*, 3550-3556.